Modelling, Measurement and Control C
Vol. 79, No. 3, September, 2018, pp. 90-97
Journal homepage: http://iieta.org/Journals/MMC/MMC_C

Design of ventilated cross flow heat sinks

Michele Trancossi[1*], Jose Pascoa[2]

[1] Sheffield Hallam University, Sheffield UK, Cedita-Romaero, Bucarest, RO
[2] Universitade da Beira Interior, Covilla, PT

Corresponding Author Email: mtrancossi@gmail.com

https://doi.org/10.18280/mmc_c.790305

Received: 15 March 2018
Accepted: 22 May 2018

Keywords:
heat sink, cross flow, lumped parameters, optimization, model

ABSTRACT

This paper presents a new design methodology of cross flow ventilated heat sinks. An accurate design of both finned and circular pin system with inline configuration has been produced. The model is based on the well tested experimental lumped parameter analysis of cross-flow heat exchangers by Gnielinski. The presented method is intended to support the design of heat sinks with well defined performances of cross flow ventilated heat sinks. An evaluation of the physical properties of the sink is performed and different cases are calculated. They allow comparing the performance in terms of both geometrical parameters of the exchanger and air speed. An effective model of the equations is produced and on this basis a multi-objective optimization is performed.

1. INTRODUCTION

1.1 First law analysis

This work derives from a former study on an innovative mathematical model of a cross flow heat exchanger under transient conditions by Dumas and Trancossi [1-3]. They have studied both the case of traditional crossflow heat exchangers and the case of a heat pipes based heat exchanger. The present paper takes the move from this theoretical research activity which has been developed to allow a reduction of the heat shocks that may appear in a cement plant that uses irregular fuel based on industrial wastes which were rich in terms of rubber.

Spiga and Spiga [4] studied the two-dimensional transient behavior of gas-to-gas crossflow heat exchangers. He solved the thermal balance problem by analytical methods and determined the transient distribution of temperatures in both the core wall and the unmixed gases. This solution assumes a large wall capacitance and deduces a solution by mean of the Lapace transform method. The results are integrals of modified Bessel functions on space and time, for a transient response with any arbitrary initial and inlet conditions, in terms of the number of transfer units, capacity rate and conductance ratio.

Spiga [5-6] also produced a well working model that applies to transient temperature fields in crossflow heat exchangers with finite wall capacitance.

Mishra, Das and Sarangi [7] studied the transient temperature response of the crossflow heat exchangers with finite wall capacitance and both fluids unmixed. They focused in particular on step, ramp and exponential perturbations provided in hot fluid inlet temperature. They have also investigated the case of for perturbations provided in both temperature and flow [8] and also applied using finite difference method accounting for the effect of temperature and flow nonuniformity at different input conditions [9].

A second direction of research has been started by Bošnjaković [10] in the years before Second World War. He claimed the necessity of introducing entropy generation analysis into the analysis of heat exchangers. It is evident that heat exchangers present two sources of entropy generation. One is the heat exchange between two streams at different temperatures. The second is constituted by the viscosity effects of moving fluids. It is evident that the entropy generation rate of the viscosity phenomena is usually much smaller than the generation in the heat exchange process. Consequently friction effects are often neglected.

Bejan [11] focused on a second law analysis of heat transfer by forced convection. He studied four fundamental flow configurations: pipe flow, boundary layer over flat plate, single cylinder in cross-flow, and flow in the entrance region of a flat rectangular duct. He analyzed the combined effects of the two fundamental irreversibility components: the one caused by heat transfer along finite temperature gradients and the one caused by viscous effects. Bejan presented both the spatial distribution of irreversibility and the entropy generation profiles or maps. He concluded both that both thermal gradients and viscous effects are strong sources of irreversibility. This work is a milestone because it states that the irreversibility, which is associated with a specific convective heat transfer process, can be reduced by an accurate optimization of the geometric parameters.

Bejan [12] has formulated a more general formulation of the problem of irreversibility (entropy generation) associated with simple heat transfer processes with an accurate analysis from the local level, at one point in a convective heat transfer arrangement. He also analyzed different classic engineering components for heat exchange, such as: heat transfer augmentation techniques, heat exchanger design, and thermal insulation systems.

Kim, Lorente and Bejan [13] show the influence of the configuration of a crossflow heat exchanger on the global performance. They consider a particular exchanger architecture. The cold-side fluid is driven by natural convection in vertical round tubes connected by two reservoirs.

The hot side fluid flows perpendicularly flows in a perpendicular direction and heats the cold tubes by forced convection. They assume that the flow is laminar on both sides. The final results has been the constructal design, which consists of many tubes with identical diameter and spacing.

2. DEFINITION OF THE PROBLEM

2.1 Preliminary hypothesis

This paper presents a cross flow heat exchanger made of multiple cold tubes. The fluid on the hot side is air, the one on the cold side is water. The exchanger works on the following set of hypotheses:

physical properties of air, and heat sink are time dependent;

the external walls of the air duct are adiabatic;

The heat sink s heated or cooled by an heat source at the basis of the heat sink;

hot gas is dry air, so there is no moist air and condensation outside the tube;

heat transfer proceeds from the air to the heat sink or viceversa.

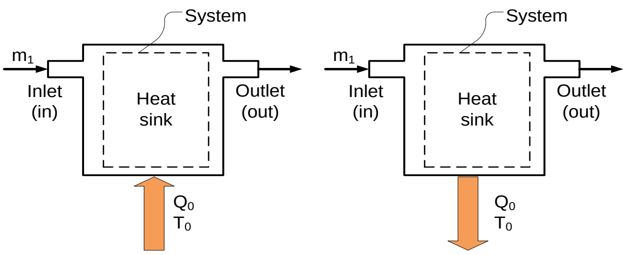

Figure 1. Schema of the heat exchange in the heat sink

2.2 General consideration about second law in heat exchange processes

The preliminary definition of the heat exchange can be performed on a reference exchanger model (Figure 1).

The control volume is initially defined around a single tube as shown in Figure 1. In the case of a heat sink the work done can be considered equal to zero. The general first law statement is consequently.

$$W - Q_0 = \dot{m} \cdot i_{in} - \dot{m} \cdot i_{out} \tag{1}$$

and the second law one is

$$0 \geq \frac{Q_0}{T_0} + \dot{m} \cdot s_{in} - \dot{m} \cdot s_{out} \tag{2}$$

The statement of equation (1) and (2) assume that the changes in kinetic energy and gravitational potential energy are negligible compared with the enthalpy changes. It allows assessing the first law equilibrium of the system. Equation (2) allows the second law assessment. It is evident that the right-hand side of equation (2) is the net rate of entropy generation in the system, S_{gen}, a quantity which is always positive and in the reversible limit equal to zero. The net rate entropy generation is evidently (according to the second law of thermodynamics) a quantity which is always positive and equal to zero in the particular case of a reversible transformation. It can be determined by the following equation:

$$S_{gen} \geq \dot{m} \cdot s_{out} - \dot{m} \cdot s_{in} - \frac{Q_0}{T_0} \tag{3}$$

Eliminating Q_0 between equation 1 and 2, it results

$$W \geq \dot{m}(i - T_0 s)_{in} - \dot{m}(i - T_0 s)_{out} \tag{4}$$

that indicates clearly that the second law is respected.

Consequently the reversibility condition is:

$$W_{\max} = \dot{m}(i - T_0 s)_{in} - \dot{m}(i - T_0 s)_{out} \tag{5}$$

in which W_{max} is the maximum achievable work.

$$W_{lost} = W_{\max} - W = T_0 \cdot S_{gen} \tag{6}$$

Equation (6) is usually named as Guy-Stodola [14, 15] theorem. In the case of an exchanger W is clearly zero and consequently the equation can be simplified. The energetic fluxes are clearly explained in Figure 2. Consequently, a coupled first and second law analysis is expected to be performed.

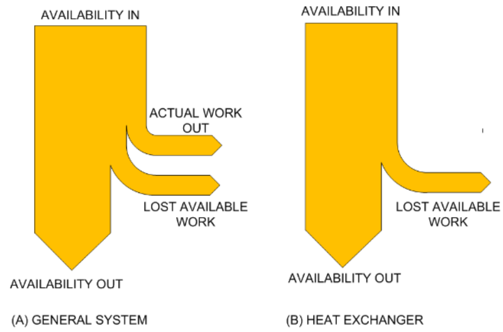

Figure 2. Energy transformation in a general mechanic system and in a heat exchanger

For the specific objectives of the heat sink design and optimization, it is possible to evidence that the work lost (destroyed) through the irreversibility of the process is proportional to the rate of entropy generation in the system.

The proportionality factor in this case is the absolute temperature T_0 of the heat reservoir (environment) with which the system exchanges heat.

Thermal design optimization requires acting in the direction of minimizing the loss of available work, and consequently elimination of irreversibility sources.

However, it is necessary to observe the industrial design of thermal systems is not usually satisfied by the simple minimization of the rate of entropy generation. It is equally important the price paid as lost available work or the price paid for the benefits over the entire lifecycle.

3. METHODOLOGY

3.1 First law analysis

Two different heat sinks designs will be adopted and compared. They are namely:

(1) Fin heat sink (Figure 3).

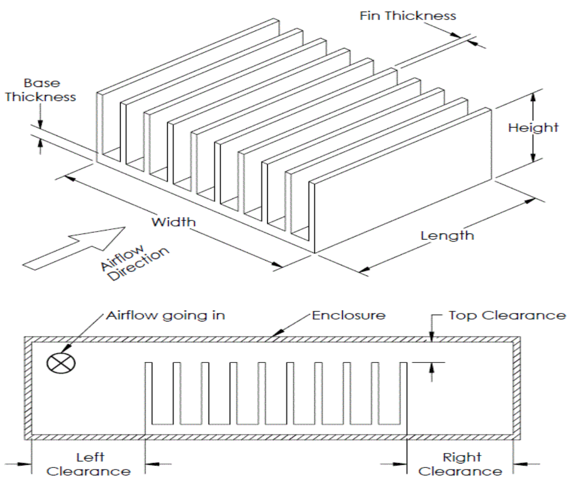

Figure 3. Fin heat sink drawing

(2) round pin heat sink (figure 4).

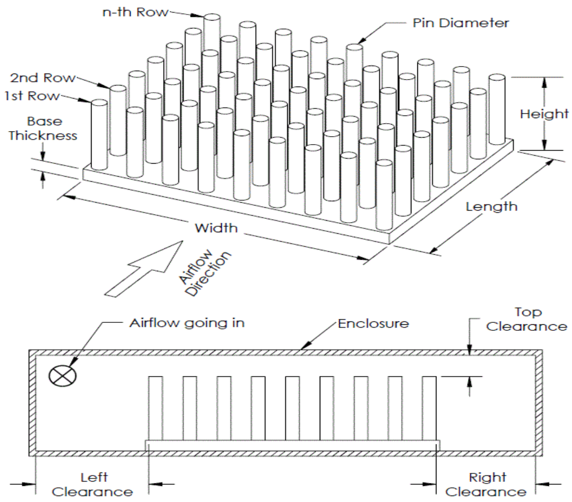

Figure 4. Round pin heat sink schematic drawing

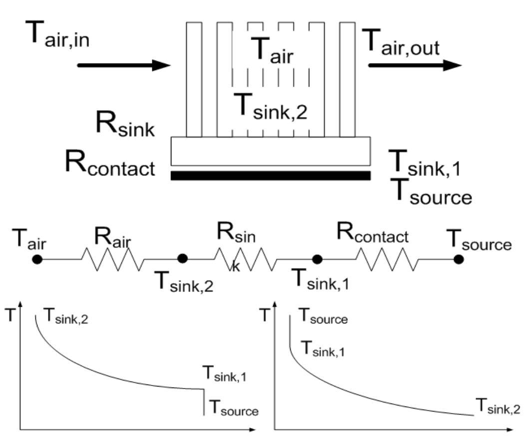

Figure 5. System schema and electric analogy with representation of cooling and heating case

A general control volume s presented in Figure 3. It consists of three different subsystems:

(1) internal flow convection (cooling water);

(2) external flow convection (air cross flow);

(3) conduction heat transfer (the walls of the tubes).

The general equation of heat exchanger is:

$$\dot{q} = \pm \frac{T_{air} - T_{source}}{R_{eq}} = \dot{m}_{air}\Delta i = \dot{m}_{air}\left(\sum i_{in} - \sum i_{out}\right) \tag{7}$$

in which

$$R_{eq} = R_{air} + R_{\text{sink}} + R_{contact} \, . \tag{8}$$

It is evident that the three resistive terms can be evaluated by considering the three heat exchange processes:

3.1.1 Contact heat transfer

$$R_{contact} = \frac{1}{h_{contact} A_{Peltier}} \tag{9}$$

in which, $h_{contact}$ depends on the materials which are placed into contact.

3.1.2 Adhesive heat transfer

Usually the electronic sources are glued to the heat sinks by adhesive materials. In particular the conductive heat transfer through the adhesive is considered included into the contact resistance.

3.1.3 Heat sink conductive heat transfer

Conduction law in the case of a finned surface can be evaluated by considering fin (or pin) efficiency.

$$\eta_0 = 1 - N\frac{A_f}{A_t}\left(1 - \eta_f\right) \tag{10}$$

in which

$$\eta_f = \frac{\tanh(mL_c)}{mL_c}$$

And

$$m = \sqrt{\frac{hP}{kA_c}}$$

In the case of a pinned

3.1.4 Air convective heat transfer

The resistance in the air side is

$$R_{air} = \frac{1}{h_{air} A_{sink}} \tag{11}$$

and the convective coefficient is

$$h_{air} = \frac{(Nu)k_{air}}{d_{out}} \, . \tag{12}$$

In this case, it is necessary to make some further considerations about the determination of the Nusselt and Reynolds numbers, because they are a function of the geometrical configuration of the exchanger.

The above calculation method applies to general problems. In particular it deals with finned heat sinks, which are probably the most common. In the case of pin heat sink other solutions can be much more effective.

3.2 Influence of the pin configuration

This section analyses the main heat sink parameters that apply thermodynamic parameters found in literature, which are summarized and defined in Annex A. The parameters relative to external fluxes are investigated and analyzed more in depth according to the models by Grimison [16], Zhukauskas [17], Incropera [18] and Gnielinski [19-21].

The ratio between the Nusselt number of a bundle of tubes and the one of a single pipe is

$$\frac{Nu_{i,bundle}}{Nu_{i,tube}} = f_a \tag{13}$$

Considering the Gnielinski experimental model, the following dimensionless dimensions have been assumed:

Transverse pitch ratio:

$$a = \frac{S_x}{D} \tag{14}$$

Longitudinal pitch ratio:

$$b = \frac{S_y}{D} \tag{15}$$

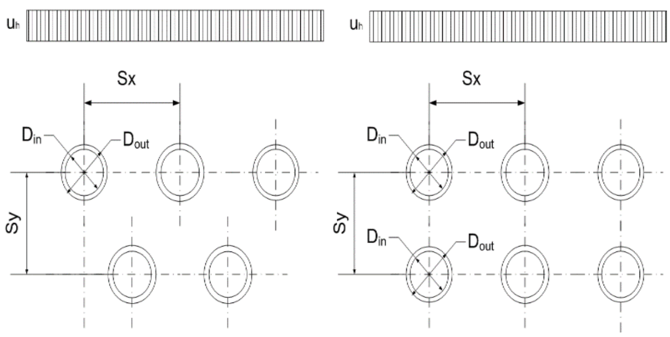

Figure 6. Staggered and inline configurations

The void ratio can be assumed by one of the following expressions:

$$b \leq 1 \rightarrow \quad \psi = 1 - \frac{\pi}{4a} \tag{16}$$

$$b < 1 \rightarrow \quad \psi = 1 - \frac{\pi}{4ab}. \tag{17}$$

It can be assumed a tube bundle with a dimensionless longitudinal pitch ratio greater than one, and consequently ψ is given by equation (14). It assumes only positive values for $a > \pi / 4$ and is always less than one.

Reynolds number of a tube bundle is:

$$Re_{bundle} = \frac{\rho_{air} u_{air} D_{pin}}{\psi \cdot \mu_{air}} = \frac{1}{\psi} \cdot Re_{pin} \tag{18}$$

In the case of an inline arrangement the main parameter is:

$$f_a = 1 + \frac{0.7}{\psi^{1.5}} \cdot \frac{(b/a - 0.3)}{(b/a + 0.7)^2} \tag{19}$$

where ψ can be determined by eqn. 18. The most interesting case is the one in which $a = b$ and the arrangement factor results:

$$f_a = 1 + \frac{1.96a}{11.56a - 9.075} \tag{20}$$

4. CALCULATIONS

The calculation model has been implemented into Scilab [10]. In order to allow an effective comparison with literature it has been assumed the following designs.

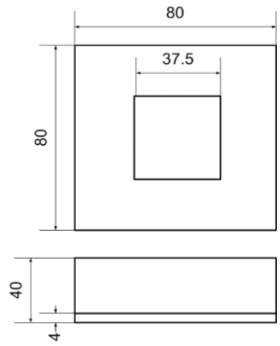

Figure 7. Dimensions of heat sink and heat source

A thermal adhesive substrate to link the sink to the heat source has been considered. In particular an epoxi-based thermal substrate has been considered (*$R_{interface}$=1,67K/W*) with a thickness of 1mm. It has been assumed that the sink is placed in a duct with the same dimensions of the sink. The airspeed has been considered of 1m/s and the inlet air temperature has been considered to be 20°C. Energy released by the heating source is 100 W.

5. RESULTS

Table 1. General characteristics of pin heat sinks

Material	**Al 6063-T6**	**Ambient Temperature**	**20 °C**
Width	80 mm	Heat to Dissipate	100 W
Length	80 mm	Width of Heat Source	37.5 mm
Height	40 mm	Length of Heat Source	37.5 mm
Base Thickness	4 mm	Top Clearance	10.0 mm
Pin Diameter	2 mm	Left Clearance	10.0 mm
		Right Clearance	10.0 mm

Different sink geometries have been considered and the properties have been reported in Table 1, 2, and 3.

The results have been presented in term of thermal resistance (Figure 8), average base temperature of the (Figure 9), and pressure drop of air (Figure 10).

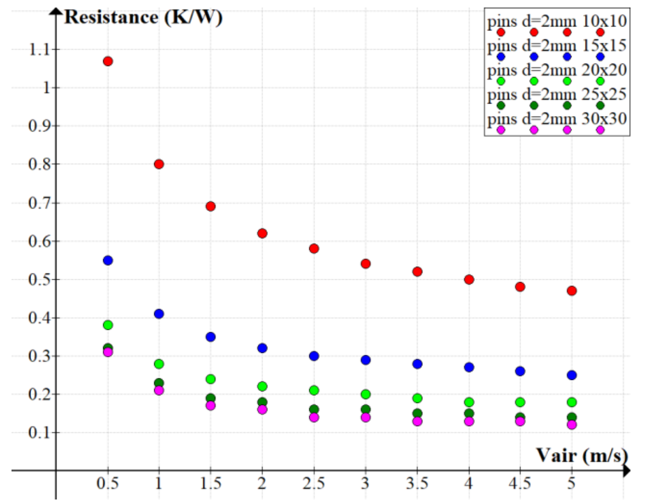

Figure 8. Thermal resistance of the pin heat sink in different square configurations

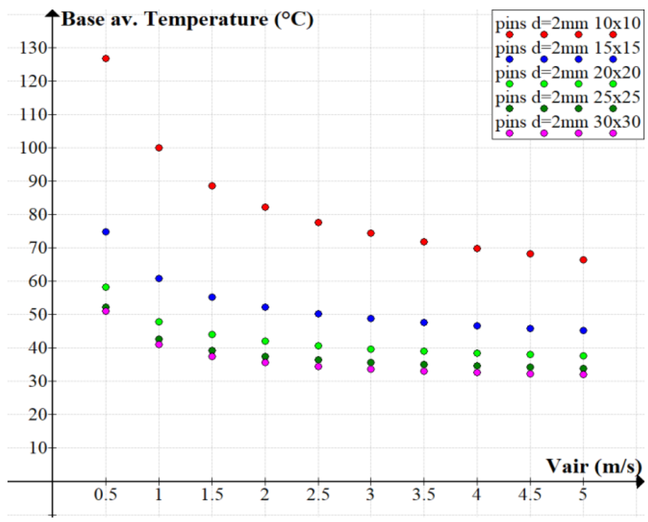

Figure 9. Average base temperature of the pin heat sink in different square configurations

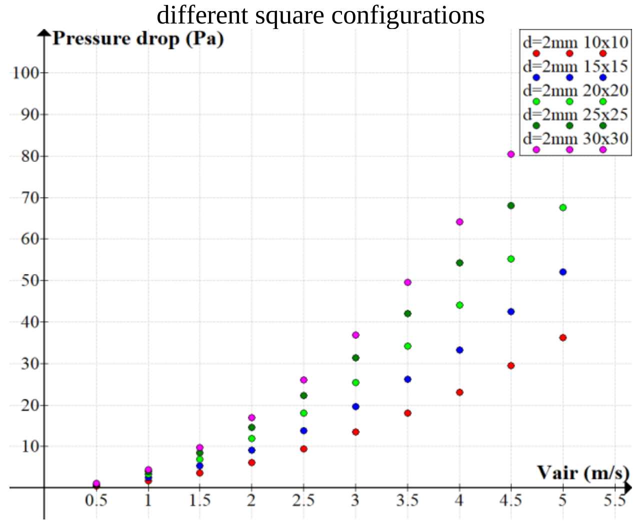

Figure 10. Pressure drop of air through the pin heat sink in different square configurations

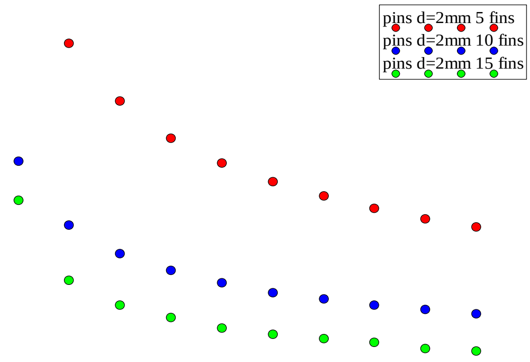

Figure 11. Thermal resistance of the fin heat sink in different configurations

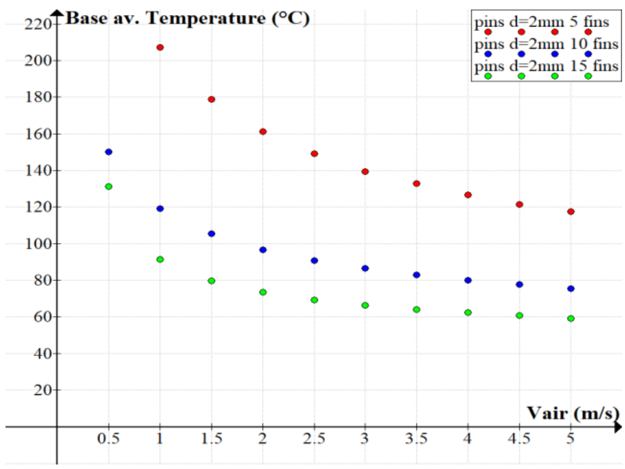

Figure 12. Average base temperature of the fin heat sink in different configurations

Table 2. General characteristics of fin heat sinks

Material	Al 6063-T6	Ambient Temperature	20 °C
Width	80 mm	Heat to Dissipate	100 W
Length	80 mm	Width of Heat Source	37.5 mm
Height	40 mm	Length of Heat Source	37.5 mm
Base Thickness	4 mm	Top Clearance	10.0 mm
Fin Thickness	2 mm	Left Clearance	10.0 mm
		Right Clearance	10.0 mm

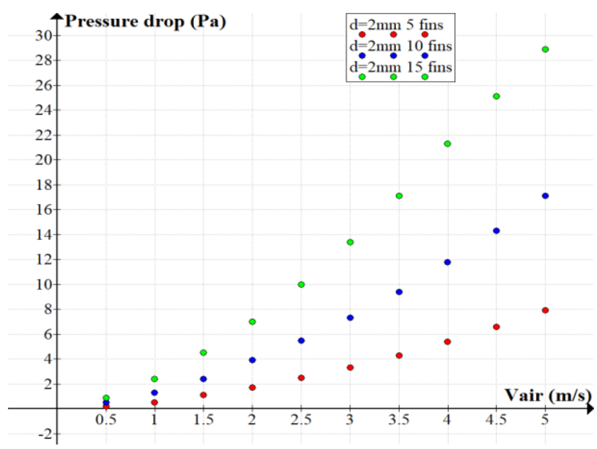

Figure 13. Pressure drop of air through the pin heat sink in different square configurations

The second tested configuration is a finned heat sink with a fin thickness of 2 mm (Table 2).

The results have been presented in term of thermal resistance (Figure 11), average base temperature of the (Figure 12), and pressure drop of air (Figure 13).

The third configuration, which has been tested, is a finned heat sink with a fin thickness of 1 mm (Table 3).

Table 3. General characteristics of finned heat sinks

Material	Al 6063-T6	Ambient Temperature	20 °C
Width	80 mm	Heat to Dissipate	100 W
Length	80 mm	Width of Heat Source	37.5 mm
Height	40 mm	Length of Heat Source	37.5 mm
Base Thickness	4 mm	Top Clearance	10.0 mm
Fin Thickness	1 mm	Left Clearance	10.0 mm
		Right Clearance	10.0 mm

The results for multiple configurations have been presented in tems of thermal resistance in Figure 14.

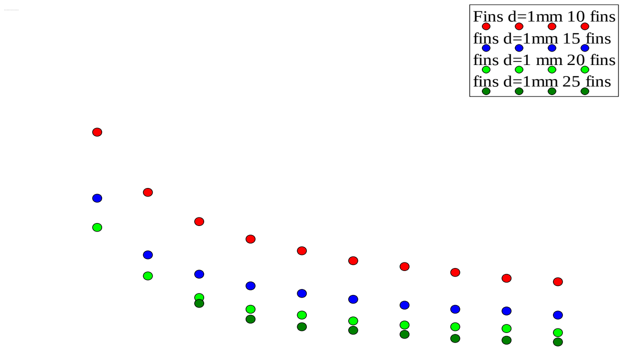

Figure 14. Thermal resistance of the fin heat sink in different configurations

The results show clearly that round pin heat sinks present much better performance with respect to fin heat sinks. In addition, it has been possible to evaluate the temperature distribution in the heat sink.

6. COMPARATIVE ANALYSIS

A comparison of a finned and a round pin heat sink (Figure 15) with comparable dimensions is presented in Figure 16.

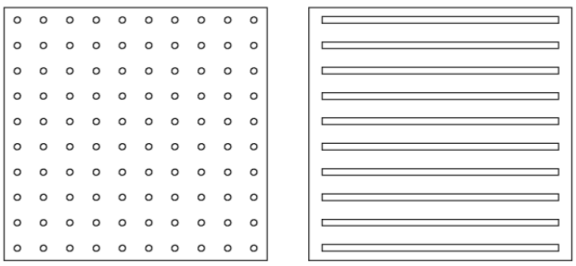

Figure 15. Compared samples in which the thickness of the fin is equal to the diameter of the pins

The general data and main parameters for the compared heat sinks are reported in Table 4.

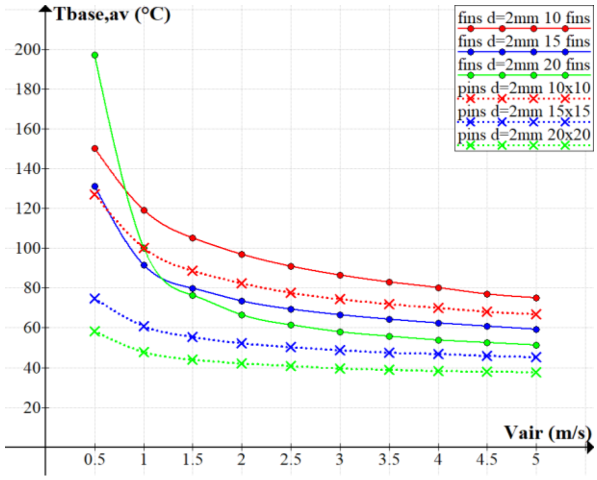

Figure 16. Comparison between finned and pin heat sinks in terms of heat dissipation capability

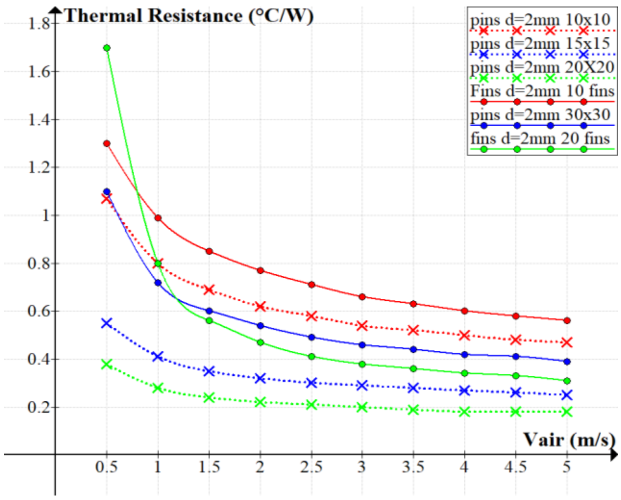

Figure 17. Thermal resistance comparison

Table 4. General characteristics of the heat sinks

Material	Al 6063-T6	Ambient Temperature	20 °C
Width	80 mm	Heat to Dissipate	100 W
Length	80 mm	Width of Heat Source	37.5 mm
Height	40 mm	Length of Heat Source	37.5 mm
Base Thickness	4 mm	Top Clearance	10.0 mm
Fin Thickness	2 mm	Left Clearance	10.0 mm
Pin diameter	2 mm	Right Clearance	10.0 mm

Figure 16 shows clearly the much higher cooling efficiency of the pin heat sinks with respect to the ones with fins.

In particular, it can be observed that the distance between successive fins cannot be arbitrary reduced, because of the concomitant effects of mutual irradiation and transition between forced convection and natural convection at low speeds. It is evident that the density of pin heat sink can be much higher with respect to the finned ones. The thermal resistance is consequently much higher in case of pin heat sinks with respect to finned ones.

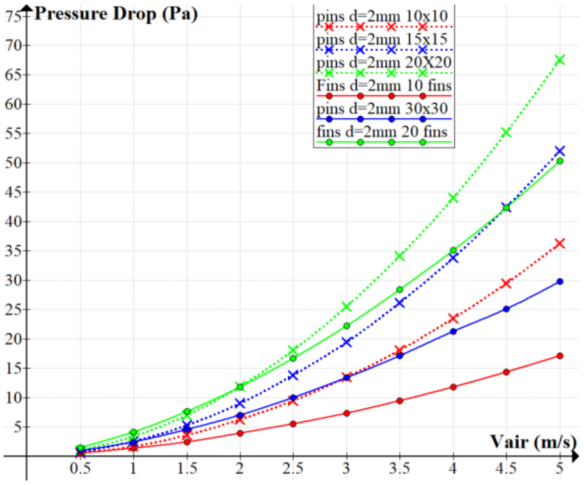

Figure 18. Pressure drops comparison

On the other side it is also evident that pressure drops are lower in the case of finned heat sinks.

7. CONCLUSIONS

This paper presents a model that allows supporting and optimizing heat sinks for the specific needs. The results have been compared against leading online tool for the design of finned heat sinks for electronic cooling [23] with a very good accordion. The difference in terms of thermal resistance and temperature in the basis did no exceed 1.5% demonstrating clearly the robustness of the algorithm. It has been demonstrated that heat sinks with fins can be preferred when the goal is not the minimization of the heat source temperature but the reduction of the pressure drops. On the other side pin heat sinks can be preferred when the key objective is the minimization of the temperature of the heat source because they ensure a much higher heat exchange performance. In addition, it has been verified that finned heat sinks must be necessarily designed keeping a certain attention to the distance between the sinks. At low air speeds, heat transfer performances degrade when the distance between the fins is too low.

REFERENCES

[1] Dumas A, Trancossi M. (2009). A mathematical based design methodology for crossflow heat exchangers. In ASME 2009 International Mechanical Engineering Congress and Exposition 1159-1165. American Society of Mechanical Engineers.

[2] Dumas A, Trancossi M. (2009). Application of heat pipes to the uniformation of thermal fluxes in industrial exhausts. In ASME 2009 International Mechanical Engineering Congress and Exposition 305-312. American Society of Mechanical Engineers.

[3] Dumas A, Trancossi M. (2009). Design of exchangers based on heat pipes for hot exhaust thermal flux, with the capability of thermal shocks absorption and low level energy recovery 2009-01-3074. SAE Technical Paper.

[4] Spiga G, Spiga M. (1987). Two-dimensional transient solutions for crossflow heat exchangers with neither gas mixed. Journal of Heat Transfer 109(2): 281-286.

[5] Spiga M, Spiga G. (1988). Transient temperature fields in crossflow heat exchangers with finite wall capacitance. Journal of heat transfer 110(1): 49-53.

[6] Spiga M, Spiga G. (1992). Step response of the crossflow heat exchanger with finite wall capacitance. International Journal of Heat and Mass Transfer 35(2): 559-565.

[7] Mishra M, Das PK, Sarangi S. (2004). Transient behavior of crossflow heat exchangers with longitudinal conduction and axial dispersion. Journal of Heat Transfer 126(3): 425-433.

[8] Mishra M, Das PK, Sarang, S. (2006). Transient behaviour of crossflow heat exchangers due to perturbations in temperature and flow. International Journal of Heat and Mass Transfer 49(5-6): 1083-1089.

[9] Mishra M, Das P.K, Sarangi S. (2004). Transient behavior of crossflow heat exchangers with longitudinal conduction and axial dispersion. Journal of Heat Transfer 126(3): 425-433.

[10] Bosnjakovic F. (1938). Kampf den nichtumkehrbarkeiten. Arch. Waermewirtsch 19: 1-2.

[11] Bejan A. (1979). A study of entropy generation in fundamental convective heat transfer. Journal of Heat Transfer, 101(4): 718-725.

[12] Bejan A. (1980). Second law analysis in heat transfer. Energy 5(8-9): 720-732.

[13] Kim Y, Lorente S, Bejan A. (2010). Constructal multi-tube configuration for natural and forced convection in cross-flow. International Journal of Heat and Mass Transfer 53(23-24): 5121-5128.

[14] Kestin J. (1979). A course in thermodynamics 1. CRC Press.

[15] Kestin J. (1980). Availability: the concept and associated terminology. Energy 5(8-9): 679-692.

[16] Grimison ED. (1937). Correlation and utilization of New Data on Flow Resistance nd Heat Transfer for Cross Flow of Gases Over Tube Banks, Transactions of the ASME 59: 583-594.

[17] Zhukauskas A, Ulinskas R. (1988). Heat Transfer in Tube Banks in Crossflow. Hemisphere Publishing Corporation. New York, NY.

[18] Bergman TL, Incropera FP, DeWitt DP, Lavine AS. (2011). Fundamentals of heat and mass transfer. John Wiley & Sons.

[19] Gnielinski V. (1975). Neue Gleichungen für den Wärme- und den Stoffübergang in turbulent durchströmten Rohren und Kanälen. Forschung im Ingenieurwesen A 41(1): 8-16.

[20] Gnielinski V. (1975). Berechnung mittlerer Wärme-und Stoffübergangskoeffizienten an laminar und turbulent überströmten Einzelkörpern mit Hilfe einer einheitlichen Gleichung. Forschung im Ingenieurwesen A 41(5): 145-153.

[21] Gnielinski V. (1979). Equations for calculating heat transfer in single tube rows and banks of tubes in transverse flow. Int. Chem. Eng.;(United States) 19(3).

[22] Scilab Enterprises. (2015). Scilab 5.5.2 - Free and Open Source software for numerical computation. Scilab Enterprises. Orsay. France 3.

[23] Heat Sink Calculator (retrieved April 2018). https://www.heatsinkcalculator.com/

NOMENCLATURE

A	Area [m^2]

D	Diameter [m]
L, l	length [m]
T	temperature [K]
H	convection coefficient [W/ (m^2K)]
K	thermal conductivity [W/ (mK)]
Q	thermal flux for unity of surface [J/m^2]
t	time [min]
U	velocity [m/s]; [m/min]
W	Work [J]

Greek symbols

μ	Dynamic viscosity [Ns/m^2]
N	kinematic viscosity [m2 /s]
P	density [kg/m^3]

Dimensionless numbers

Fa	arrangement factor [-]
ψ	Void ratio [-]
Re	Reynolds Number
Pr	Prandtl Number [-]
St	Stanton Number [-]
a	Transversal pitch ratio [-]